Modeling, Identification and Control, Vol. 33, No. 3, 2012, pp. 87–97, ISSN 1890–1328

Optimal passive-damping design using a decentralized velocity-feedback H_∞ approach

F. Palacios-Quiñonero [1] J. Rubió-Massegú [1] J.M. Rossell [1] H.R. Karimi [2]

[1] *CoDAlab. Department of Applied Mathematics III, Universitat Politècnica de Catalunya (UPC)*
Av. Bases de Manresa 61-73, 08242-Manresa, Barcelona, Spain
E-mail: francisco.palacios@upc.edu, josep.rubio@upc.edu, josep.maria.rossell@upc.edu

[2] *Department of Engineering, Faculty of Engineering and Science*
University of Agder (UiA), N-4898 Grimstad, Norway
E-mail: hamid.r.karimi@uia.no

Abstract

In this work, a new strategy to design passive energy dissipation systems for vibration control of large structures is presented. The method is based on the equivalence between passive damping systems and fully decentralized static velocity-feedback controllers. This equivalence allows to take advantage of recent developments in static output-feedback control design to formulate the passive-damping design as a single optimization problem with Linear Matrix Inequality constraints. To illustrate the application of the proposed methodology, a passive damping system is designed for the seismic protection of a five-story building with excellent results.

Keywords: Decentralized Control; Structural Vibration Control; Static Output-feedback; Optimal Passive Damping

1 Introduction

Over the last decades, the design of *energy dissipation systems* (EDSs) to reduce the dynamic response of large structures has become a very active research field. Good examples of the advances in this field are the numerous *structural vibration control* (SVC) systems proposed to mitigate the seismic vibrational response of large buildings and other civil structures. These SVC systems include different kinds of passive, active, and semiactive actuation devices, and a wide variety of control methodologies and techniques [Spencer and Nagarajaiah (2003), Ikeda (2009), Li and Huo (2010)].

To deal with the challenging problems associated to the design of these highly complex control systems, recent developments in control theory have been incorporated to SVC. This makes it possible to consider some relevant practical issues such as nonlinear actuation devices, parameter uncertainties, wireless implementation of communication systems, actuator saturation, actuation and sensor failures, structural information constraints, limited frequency domain, or multistructure systems [Du and Lam (2006), Swartz and Lynch (2009), Chen et al. (2010), Palacios-Quiñonero et al. (2011), Zhang et al. (2011b), Palacios-Quiñonero et al. (2012a,b)].

Passive energy dissipation devices, such as viscous fluid dampers, viscoelastic dampers, friction dampers, etc., are simple, compact, and reliable. Effective and relatively inexpensive EDSs for vibration control of large structures can be designed by implementing a set of passive dampers at suitable locations of the structure.

One of the main problems in the design of passive EDSs consists in determining the damping capacity of the different dampers. Traditionally, this prob-

doi:10.4173/mic.2012.3.1

lem has been solved through a trial-and-error procedure, and assuming that the dampers are identical. In general, passive dampers exhibit a nonlinear behavior. However, approximate linear models can be used in the design of passive EDSs. For viscous fluid dampers, the damping force can be considered proportional to the velocity. In this case, the passive damping system is equivalent to a fully decentralized static velocity-feedback control system, and the powerful design strategies of feedback control can be used to define a systematic procedure to compute the passive damping constants. This line of work has been successfully used in the early work of Gluck et al. (1996), and extended in Agrawal and Yang (1999) and Yang et al. (2002).

It has to be highlighted, however, that this new approach is not exempt of difficulties, which are mainly related to the computational cost of designing decentralized static output-feedback controllers. For example, the design methodology proposed in Agrawal and Yang (1999) is based on the linear quadratic regulator (LQR) theory and the decentralized static output-feedback controller is computed by means of an iterative procedure, which requires solving complex matricial equations at each step. The methodology proposed in Yang et al. (2002) uses the more advanced H_∞ and H_2 control theories and Linear Matrix Inequality (LMI) formulations but, again, the decentralized static output-feedback controller is computed by means of an iterative procedure which, in this case, requires solving an optimization problem with LMI constraints at each step.

Recently, an effective strategy to compute static output-feedback controllers was presented by Rubió-Massegú et al. (2012a). This strategy is based on a simple transformation of the LMI variables that allows computing structured output-feedback control gain matrices by solving a single optimization problem with LMI constraints. The objective of the present paper is to apply these recent advances in static output-feedback control in the design of passive EDSs for structural vibration control of large structures. To illustrate the application of the proposed methodology, a passive EDS is designed for the seismic protection of a five-story building with excellent results.

The rest of the paper is organized as follows. Section 2 is devoted to discuss the equivalence between passive linear damping systems and fully decentralized static velocity-feedback controllers. For clarity and notational simplicity, the main ideas are presented through a three-degree-of-freedom mass-spring-damper system. In Section 3, the new methodology to compute decentralized static output-feedback H_∞ controllers is summarized. In Section 4, a passive EDS and a state-feedback H_∞ controller are designed for seismic protection of a five-story building. Numerical simulations of the free and controlled vibrational responses together with the corresponding control actions are presented and compared. Finally, in Section 5, conclusions are drawn and some directions for future work are proposed.

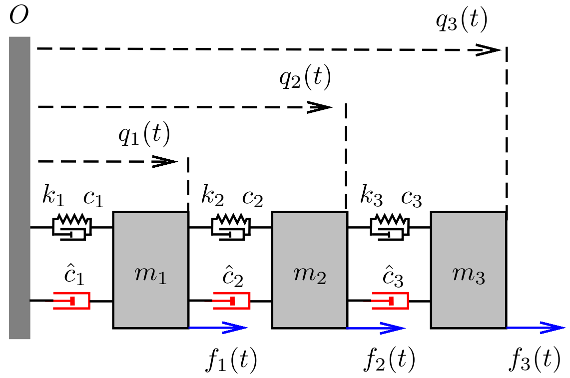

Figure 1: Mechanical system with passive dampers for vibrational response mitigation

2 Decentralized velocity-feedback control and passive dampers

Let us consider the mechanical system schematically depicted in Figure 1. For $1 \le i \le 3$, m_i denote the masses; c_i and k_i are, respectively, the structural damping and stiffness coefficients; $q_i(t)$ is the displacement of the ith mass with respect to the reference frame O; and $f_i(t)$ are the external force disturbances. Moreover, a second set of linear dampers with damping constants $\hat{c}_i$ have been included. The objective of this additional damping system is helping to mitigate the vibrational response induced by the external disturbances.

The system motion can be described by the second-order model

$$M\ddot{q}(t) + \left(C + \hat{C}\right)\dot{q}(t) + Kq(t) = f(t), \qquad (1)$$

where

$$q(t) = [q_1(t), q_2(t), q_3(t)]^T \qquad (2)$$

is the vector of displacements, M is the *mass matrix*

$$M = \begin{bmatrix} m_1 & 0 & 0 \\ 0 & m_2 & 0 \\ 0 & 0 & m_3 \end{bmatrix}, \qquad (3)$$

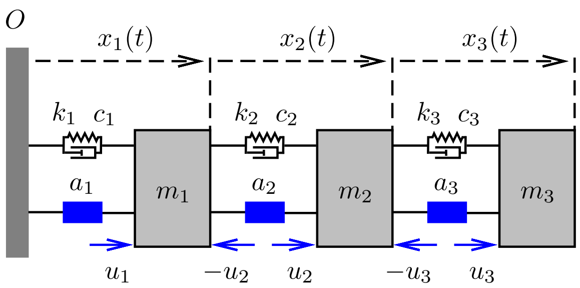

Figure 2: Mechanical system with active force actuation devices

C is the *structural damping matrix*

$$C=\begin{bmatrix} c_1+c_2 & -c_2 & 0\\ -c_2 & c_2+c_3 & -c_3\\ 0 & -c_3 & c_3\end{bmatrix}, \tag{4}$$

$\hat{C}$ is the *vibration control damping matrix*

$$\hat{C}=\begin{bmatrix} \hat{c}_1+\hat{c}_2 & -\hat{c}_2 & 0\\ -\hat{c}_2 & \hat{c}_2+\hat{c}_3 & -\hat{c}_3\\ 0 & -\hat{c}_3 & \hat{c}_3\end{bmatrix}, \tag{5}$$

K is the *structural stiffness matrix*

$$K=\begin{bmatrix} k_1+k_2 & -k_2 & 0\\ -k_2 & k_2+k_3 & -k_3\\ 0 & -k_3 & k_3\end{bmatrix}, \tag{6}$$

and

$$f(t)=[f_1(t),f_2(t),f_3(t)]^T \tag{7}$$

is the vector of external force disturbances. Matrices M, C, and K determine the structural characteristics of the system and are supposed to have given values. The objective of the present work is to design a passive damping system to reduce the vibrational response induced by the external disturbance $f(t)$. In terms of the system matrices, the objective is to find an effective strategy to determine a suitable matrix $\hat{C}$.

Let us now consider the mechanical system displayed in Figure 2, where the blue rectangles a_i, $1\leq i\leq 3$, represent ideal active force-actuation devices, which produce actuation forces $u_i(t)$ as indicated in the figure.

Using the vector of control forces

$$u(t)=[u_1(t),u_2(t),u_3(t)]^T \tag{8}$$

and the *control location matrix*

$$T_u=\begin{bmatrix} 1 & -1 & 0\\ 0 & 1 & -1\\ 0 & 0 & 1\end{bmatrix}, \tag{9}$$

the motion of the actively controlled system can be described by the following second-order model:

$$M\ddot{q}(t)+C\dot{q}(t)+Kq(t)=f(t)+f_u(t), \tag{10}$$

where $f_u(t)$ is the vector of actuation forces, which can be expressed in the form

$$f_u(t)=T_u u(t). \tag{11}$$

Next, we consider the vector of relative displacements

$$x_r(t)=[x_1(t),x_2(t),x_3(t)]^T, \tag{12}$$

where

$$\begin{cases} x_1(t)=q_1(t),\\ x_2(t)=q_2(t)-q_1(t),\\ x_3(t)=q_3(t)-q_2(t).\end{cases} \tag{13}$$

If we design a state-feedback controller to drive the actuation devices a_i, the control actions can be computed in the form

$$u(t)=\begin{bmatrix} g_{11} & g_{12} & g_{13} & g_{14} & g_{15} & g_{16}\\ g_{21} & g_{22} & g_{23} & g_{24} & g_{25} & g_{26}\\ g_{31} & g_{32} & g_{33} & g_{34} & g_{35} & g_{36}\end{bmatrix}\begin{bmatrix} x_1(t)\\ x_2(t)\\ x_3(t)\\ \dot{x}_1(t)\\ \dot{x}_2(t)\\ \dot{x}_3(t)\end{bmatrix}. \tag{14}$$

Obviously, a practical implementation of this controller would require sensors of relative position and relative velocity, and also a full communication system. For a static velocity-feedback controller, the control actions can be computed in the form

$$u(t)=\begin{bmatrix} g_{11} & g_{12} & g_{13}\\ g_{21} & g_{22} & g_{23}\\ g_{31} & g_{32} & g_{33}\end{bmatrix}\begin{bmatrix} \dot{x}_1(t)\\ \dot{x}_2(t)\\ \dot{x}_3(t)\end{bmatrix}. \tag{15}$$

A practical implementation of this second control strategy requires sensors of relative velocity and also a full communication system. Finally, for a fully decentralized velocity-feedback controller, the control actions can be computed in the form

$$u(t)=\begin{bmatrix} u_1(t)\\ u_2(t)\\ u_3(t)\end{bmatrix}=\begin{bmatrix} g_{11} & 0 & 0\\ 0 & g_{22} & 0\\ 0 & 0 & g_{33}\end{bmatrix}\begin{bmatrix} \dot{x}_1(t)\\ \dot{x}_2(t)\\ \dot{x}_3(t)\end{bmatrix}. \tag{16}$$

Let us suppose that a controller with the structure given in eq. (16) is available and, moreover, that all the elements g_{ii} are negative. In this case, we can write

$$\hat{c}_i=-g_{ii},\quad 1\leq i\leq 3, \tag{17}$$

and the vector of control forces takes the following form:

$$f_u(t)=\begin{bmatrix} 1 & -1 & 0\\ 0 & 1 & -1\\ 0 & 0 & 1\end{bmatrix}\begin{bmatrix} -\hat{c}_1 & 0 & 0\\ 0 & -\hat{c}_2 & 0\\ 0 & 0 & -\hat{c}_3\end{bmatrix}\begin{bmatrix} \dot{x}_1(t)\\ \dot{x}_2(t)\\ \dot{x}_3(t)\end{bmatrix}. \tag{18}$$

Finally, from eq. (13), we get

$$f_u(t) = -\begin{bmatrix} \hat{c}_1 & -\hat{c}_2 & 0 \\ 0 & \hat{c}_2 & -\hat{c}_3 \\ 0 & 0 & \hat{c}_3 \end{bmatrix} \begin{bmatrix} \dot{q}_1(t) \\ \dot{q}_2(t) - \dot{q}_1(t) \\ \dot{q}_3(t) - \dot{q}_2(t) \end{bmatrix}$$
$$= -\begin{bmatrix} \hat{c}_1 + \hat{c}_2 & -\hat{c}_2 & 0 \\ -\hat{c}_2 & \hat{c}_2 + \hat{c}_3 & -\hat{c}_3 \\ 0 & -\hat{c}_3 & \hat{c}_3 \end{bmatrix} \begin{bmatrix} \dot{q}_1(t) \\ \dot{q}_2(t) \\ \dot{q}_3(t) \end{bmatrix}. \quad (19)$$

In summary, the vector of actuation forces can be written in the form

$$f_u(t) = -\hat{C}\dot{q}(t) \quad (20)$$

and, consequently, the values of the damping coefficients $\hat{c}_i$ can be obtained from the decentralized velocity-feedback control gain matrix as indicated in eq. (17).

Remark 1 Obviously, the discussed method can only be applied if we are able to compute effective decentralized velocity-feedback controllers.

3 Design of static output-feedback H_∞ controllers

Let us consider the system

$$\mathcal{S}: \begin{cases} \dot{x}(t) = Ax(t) + Bu(t) + Ew(t), \\ y(t) = C_y\, x(t), \\ z(t) = C_z x(t) + D_z u(t), \end{cases} \quad (21)$$

where $x(t) \in \mathbb{R}^n$ is the state, $u(t) \in \mathbb{R}^m$ is the control input, $w(t) \in \mathbb{R}^r$ is the disturbance input, $y(t) \in \mathbb{R}^p$ is the observed output, and $z(t) \in \mathbb{R}^{n_z}$ is the controlled output. A, B, E, C_y, C_z, and D_z are known, real and constant matrices of appropriate dimensions. A static output-feedback controller has the form

$$u(t) = Gy(t), \quad (22)$$

where G is a constant control gain matrix. From eqs. (21) and (22), we obtain the following closed-loop system:

$$\mathcal{S}_{CL}: \begin{cases} \dot{x}(t) = \bar{A}_G\, x(t) + Ew(t), \\ z(t) = \bar{C}_G\, x(t), \end{cases} \quad (23)$$

where

$$\bar{A}_G = A + BGC_y, \quad \bar{C}_G = C_z + D_z G C_y. \quad (24)$$

The H_∞ control approach considers the largest energy gain from disturbance to controlled output

$$\gamma_G = \sup_{\|w\|_2 \neq 0} \frac{\|z\|_2}{\|w\|_2}, \quad (25)$$

where $w(t)$ and $z(t)$ denote, respectively, the disturbance input and controlled output in eq. (21), and $\|\cdot\|_2$ is the usual continuous 2-norm

$$\|f\|_2 = \left[\int_0^\infty \{f(t)\}^T f(t)\, dt \right]^{1/2}. \quad (26)$$

The control design objective is to obtain a gain matrix $\tilde{G}$ which simultaneously produces a stable closed-loop matrix $\bar{A}_{\tilde{G}}$ and an optimally small value $\gamma_{\tilde{G}}$. Using the closed-loop transfer function from the disturbance $w(t)$ to the controlled output $z(t)$

$$T_G(s) = \bar{C}_G(sI - \bar{A}_G)^{-1}E, \quad (27)$$

the value $\gamma_{\tilde{G}}$ can be expressed as the H_∞-norm of $T_{\tilde{G}}$

$$\gamma_{\tilde{G}} = \|T_{\tilde{G}}(s)\|_\infty = \sup_\omega \bar{\sigma}[T_{\tilde{G}}(j\omega)], \quad (28)$$

where $\bar{\sigma}[\cdot]$ denotes the maximum singular value.

According to the *Bounded Real Lemma* [Boyd et al. (1994)], for a prescribed $\gamma > 0$, the following two statements are equivalent:

1. $\|T_G(s)\|_\infty < \gamma$, *and* $\bar{A}_G$ *is stable.*

2. *There exists a symmetric positive-definite matrix* $X \in \mathbb{R}^{n\times n}$ *such that the matrix inequality*

$$\begin{bmatrix} \bar{A}_G X + X\bar{A}_G^T + \gamma^{-2}EE^T & * \\ \bar{C}_G X & -I \end{bmatrix} < 0 \quad (29)$$

holds, where $*$ *denotes the transpose elements in the symmetric positions.*

From eqs. (24) and (29), we obtain the nonlinear matrix inequality (MI–A) displayed in Figure 3, which can be converted into the following LMI:

$$\begin{bmatrix} AX + XA^T + BY + Y^T B^T + \eta EE^T & * \\ C_z X + D_z Y & -I \end{bmatrix} < 0 \quad (30)$$

by introducing the new variables

$$Y = GC_y X, \qquad \eta = \gamma^{-2}. \quad (31)$$

The continuous-time output-feedback H_∞ control design problem can now be formulated as the following optimization problem:

$$\begin{cases} \text{maximize } \eta \\ \text{subject to } X > 0,\ \eta > 0 \text{ and the LMI in eq. (30)}, \end{cases} \quad (32)$$

where the matrices X and Y are the optimization variables. If an optimal value η_{opt} is attained for the matrices $\tilde{X}$, $\tilde{Y}$, and a control matrix $\tilde{G}$ satisfying

$$\tilde{Y} = \tilde{G} C_y \tilde{X} \quad (33)$$

$$\begin{bmatrix} AX + XA^T + BGC_yX + XC_y^TG^TB^T + \gamma^{-2}EE^T & * \\ C_zX + D_zGC_yX & -I \end{bmatrix} < 0 \quad \text{(MI–A)}$$

$$\begin{bmatrix} AQX_{_Q}Q^T + QX_{_Q}Q^TA^T + ARX_{_R}R^T + RX_{_R}R^TA^T + BY_{_R}R^T + RY_{_R}^TB^T + \eta EE^T & * \\ C_zQX_{_Q}Q^T + C_zRX_{_R}R^T + D_zY_{_R}R^T & -I \end{bmatrix} < 0 \quad \text{(LMI–B)}$$

Figure 3: Matrix inequalities

can be determined, then the corresponding static output-feedback controller

$$u(t) = \tilde{G}y(t) \tag{34}$$

defines a stable closed-loop matrix $\bar{A}_{\tilde{G}}$ with an associated H_∞-norm

$$\gamma_{\tilde{G}} = (\eta_{\text{opt}})^{-1/2}. \tag{35}$$

Remark 2 It should be noted that eq. (33) only provides an implicit definition of the gain matrix $\tilde{G}$ and, in general, this equation can not be properly solved to obtain $\tilde{G}$.

Using a suitable set of transformations of the LMI variables, a simple and explicit formulation for the gain matrix $\tilde{G}$ can be obtained. Moreover, decentralized static output-feedback controllers can also be designed by imposing an appropriate zero–nonzero structure on the new LMI variables. Next, we summarize the main ideas of this design strategy; a detailed discussion can be found in Rubió-Masseguú et al. (2012a).

Given a full row-rank output matrix C_y with dimensions $p \times n$, $p \leq n$, we consider an $n \times (n-p)$ matrix Q, whose columns are a basis of $\text{Ker}(C_y)$; and the *Moore-Penrose pseudo-inverse* of C_y, which is given by

$$R = C_y^T(C_yC_y^T)^{-1}. \tag{36}$$

From matrices Q and R, we define the following transformations:

$$X = Q\,X_{_Q}\,Q^T + R\,X_{_R}\,R^T, \quad Y = Y_{_R}\,R^T, \tag{37}$$

where $X_{_Q}$, $X_{_R}$ are symmetric positive-definite matrices with respective dimensions $(n-p)\times(n-p)$, $p\times p$; and $Y_{_R}$ is an $m \times p$ matrix. Using the transformations given in eq. (37), the LMI in eq. (30) takes the form (LMI–B) displayed in Figure 3. If the following optimization problem

$$\begin{cases} \text{maximize } \eta \\ \text{subject to } X_{_Q} > 0,\ X_{_R} > 0,\ \eta > 0, \text{ and (LMI–B)}, \end{cases} \tag{38}$$

is solvable with an optimum value $\tilde{\eta}_{\text{opt}}$ attained by the matrices $\tilde{X}_{_Q}$, $\tilde{X}_{_R}$, and $\tilde{Y}_{_R}$, then the control matrix

$$\tilde{G} = \tilde{Y}_{_R}\left(\tilde{X}_{_R}\right)^{-1} \tag{39}$$

defines a static output-feedback controller

$$u(t) = \tilde{G}\,y(t) \tag{40}$$

with stable closed-loop matrix $\bar{A}_{\tilde{G}}$, and H_∞-norm

$$\gamma_{\tilde{G}} \leq (\tilde{\eta}_{\text{opt}})^{-1/2}. \tag{41}$$

Remark 3 Note that the expression for the output-feedback control matrix given in eq. (39) is analogous to the formulation normally used in the design of state-feedback H_∞ controllers. Structured output-feedback controllers can be designed in the usual way by taking $X_{_R}$ as a block-diagonal matrix and $Y_{_R}$ with the zero-nonzero structure desired for $\tilde{G}$.

Remark 4 The presented control design methodology can be applied to compute decentralized static velocity-feedback controllers. This fact allows implementing the ideas proposed in Section 2 in designing passive damping systems for structural vibration control.

Remark 5 Setting structural constraints on the control matrix $\tilde{G}$ implies a loss of free LMI variables, which can lead to greater γ-values and may even produce infeasibility.

Remark 6 The optimization problem in eq. (38) is a particular case of the optimization problem presented in eq. (32) with the additional constraints given in eq. (37). Hence, we will have $\eta_{\text{opt}} \geq \tilde{\eta}_{\text{opt}}$ and, consequently, $(\tilde{\eta}_{\text{opt}})^{-1/2}$ will only provide an upper bound of the H_∞-norm $\gamma_{\tilde{G}}$ as indicated in eq. (41).

4 Application to seismic protection of buildings

In this section, the ideas presented in Section 2 and Section 3 are applied to design a passive damping system for seismic protection of a five-story building. In

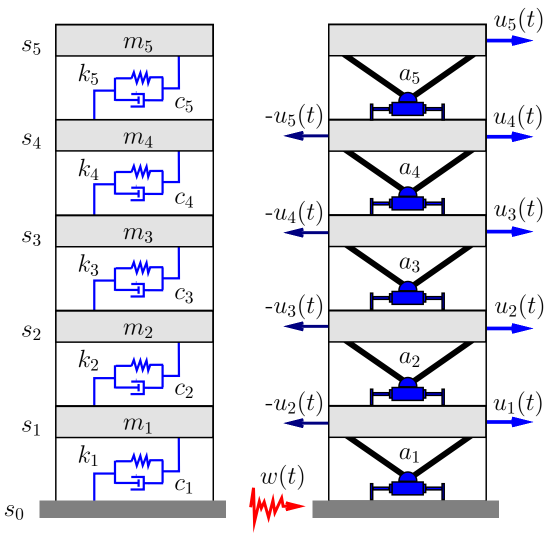

(a) Mechanical model (b) Actuation forces

Figure 4: Five story-building mechanical model, actuation forces, and external disturbance

Subsection 4.1, second-order and first-order mathematical models of the building are provided. In Subsection 4.2, a static state-feedback H_∞ controller is designed, which will be taken as a reference in the performance assessment of the proposed passive damping system. Next, in Subsection 4.3, a decentralized static output-feedback H_∞ controller is designed to compute the damping coefficients for the passive damping system. Finally, numerical simulations of the free and controlled vibrational response of the building are presented and compared in Subsection 4.4. The full-scale North–South Hachinohe 1968 seismic record is used as external disturbance in these numerical simulations.

4.1 Building model

Let us consider the five-story building schematically depicted in Figure 4. The building motion can be described by the second-order differential equation

$$M\ddot{q}(t) + C\dot{q}(t) + Kq(t) = T_u u(t) + T_w w(t), \qquad (42)$$

where M, C, and K, are the mass, damping, and stiffness matrices, respectively. The vector of displacements relative to the ground is

$$q(t) = [q_1(t), q_2(t), q_3(t), q_4(t), q_5(t)]^T, \qquad (43)$$

where $q_i(t)$, $1 \leq i \leq 5$, represents the lateral displacement of the ith story s_i with respect to the ground level s_0. We assume that, between the consecutive stories s_{i-1} and s_i, an actuation device a_i has been implemented, which exerts a control action $u_i(t)$ as indicated in Figure 4(b). The vector of control actions is

$$u(t) = [u_1(t), u_2(t), u_3(t), u_4(t), u_5(t)]^T, \qquad (44)$$

T_u is the control location matrix, $w(t)\in\mathbb{R}$ denotes the seismic ground acceleration, and T_w is the excitation location matrix. The particular values of the matrices M, C, K, T_u, and T_w used in this paper are the following:

$$M = 10^3 \times \begin{bmatrix} 215.2 & 0 & 0 & 0 & 0 \\ 0 & 209.2 & 0 & 0 & 0 \\ 0 & 0 & 207.0 & 0 & 0 \\ 0 & 0 & 0 & 204.8 & 0 \\ 0 & 0 & 0 & 0 & 266.1 \end{bmatrix}, \qquad (45)$$

$$C = 10^3 \times \begin{bmatrix} 260.2 & -92.4 & 0 & 0 & 0 \\ -92.4 & 219.6 & -81.0 & 0 & 0 \\ 0 & -81.0 & 199.5 & -72.8 & 0 \\ 0 & 0 & -72.8 & 186.7 & -68.7 \\ 0 & 0 & 0 & -68.7 & 127.4 \end{bmatrix}, \qquad (46)$$

$$K = 10^6 \times \begin{bmatrix} 260 & -113 & 0 & 0 & 0 \\ -113 & 212 & -99 & 0 & 0 \\ 0 & -99 & 188 & -89 & 0 \\ 0 & 0 & -89 & 173 & -84 \\ 0 & 0 & 0 & -84 & 84 \end{bmatrix}, \qquad (47)$$

$$T_u = \begin{bmatrix} 1 & -1 & 0 & 0 & 0 \\ 0 & 1 & -1 & 0 & 0 \\ 0 & 0 & 1 & -1 & 0 \\ 0 & 0 & 0 & 1 & -1 \\ 0 & 0 & 0 & 0 & 1 \end{bmatrix}, \; T_w = -M \begin{bmatrix} 1 \\ 1 \\ 1 \\ 1 \\ 1 \end{bmatrix}, \qquad (48)$$

where masses are in kg, damping coefficients in Ns/m, and stiffness coefficients in N/m. The mass and stiffness values in eqs. (45) and (47) are similar to those corresponding to the Kajima-Sizuoka building presented in Kurata et al. (1999); the damping matrix C has been computed as a Rayleigh damping matrix with a 2% damping ratio on the first and fifth modes [Chopra (2007)].

From the second-order model given in eq. (42), we can derive a first-order state-space model

$$S_I : \dot{x}_I(t) = A_I x_I(t) + B_I u(t) + E_I w(t), \qquad (49)$$

by taking the state vector

$$x_I(t) = \begin{bmatrix} q(t) \\ \dot{q}(t) \end{bmatrix}. \qquad (50)$$

The state matrix in eq. (49) has the structure

$$A_I = \begin{bmatrix} [0]_{5\times5} & I_5 \\ -M^{-1}K & -M^{-1}C \end{bmatrix}, \qquad (51)$$

while the control and disturbance input matrices are, respectively,

$$B_I = \begin{bmatrix} [0]_{5\times5} \\ M^{-1}T_u \end{bmatrix}, \quad E_I = \begin{bmatrix} [0]_{5\times1} \\ -[1]_{5\times1} \end{bmatrix}, \qquad (52)$$

$$A = 10^3 \times \begin{bmatrix} 0 & 0 & 0 & 0 & 0 & 0.0010 & 0 & 0 & 0 & 0 \\ 0 & 0 & 0 & 0 & 0 & 0 & 0.0010 & 0 & 0 & 0 \\ 0 & 0 & 0 & 0 & 0 & 0 & 0 & 0.0010 & 0 & 0 \\ 0 & 0 & 0 & 0 & 0 & 0 & 0 & 0 & 0.0010 & 0 \\ 0 & 0 & 0 & 0 & 0 & 0 & 0 & 0 & 0 & 0.0010 \\ -0.6831 & 0.5251 & 0 & 0 & 0 & -0.0008 & 0.0004 & 0 & 0 & 0 \\ 0.6831 & -1.0652 & 0.4732 & 0 & 0 & 0.0006 & -0.0011 & 0.0004 & 0 & 0 \\ 0 & 0.5402 & -0.9515 & 0.4300 & 0 & 0 & 0.0004 & -0.0010 & 0.0004 & 0 \\ 0 & 0 & 0.4783 & -0.8645 & 0.4102 & 0 & 0 & 0.0004 & -0.0009 & 0.0003 \\ 0 & 0 & 0 & 0.4346 & -0.7258 & 0 & 0 & 0 & 0.0004 & -0.0008 \end{bmatrix}$$

$$B = 10^{-5} \times \begin{bmatrix} 0 & 0 & 0 & 0 & 0 \\ 0 & 0 & 0 & 0 & 0 \\ 0 & 0 & 0 & 0 & 0 \\ 0 & 0 & 0 & 0 & 0 \\ 0 & 0 & 0 & 0 & 0 \\ 0.4647 & -0.4647 & 0 & 0 & 0 \\ -0.4647 & 0.9427 & -0.4780 & 0 & 0 \\ 0 & -0.4780 & 0.9611 & -0.4831 & 0 \\ 0 & 0 & -0.4831 & 0.9714 & -0.4883 \\ 0 & 0 & 0 & -0.4883 & 0.8641 \end{bmatrix}, \quad E = \begin{bmatrix} 0 \\ 0 \\ 0 \\ 0 \\ 0 \\ -1 \\ 0 \\ 0 \\ 0 \\ 0 \end{bmatrix}$$

Figure 5: System matrices of the first-order model with interstory drifts and interstory velocities as state variables

$$G_s = 10^7 \times \begin{bmatrix} 0.2610 & -0.3046 & 0.1131 & -0.1075 & -0.1084 & -0.2281 & -0.1348 & -0.0324 & -0.0356 & -0.0188 \\ -0.3488 & 0.4113 & -0.1358 & 0.2960 & -0.5236 & -0.1050 & -0.2345 & -0.1116 & -0.0276 & -0.0326 \\ 0.3801 & -0.7608 & 0.6698 & 0.0290 & -0.4281 & -0.1052 & -0.1333 & -0.1933 & -0.0355 & -0.0538 \\ 0.4170 & -0.0836 & -0.7695 & 0.7284 & -0.0265 & -0.0517 & -0.0887 & -0.1111 & -0.1612 & -0.0377 \\ 0.1032 & 0.0593 & 0.1569 & -1.0576 & 1.1411 & -0.0692 & -0.0580 & -0.0346 & -0.0827 & -0.0616 \end{bmatrix}$$

Figure 6: State-feedback gain matrix G_s

where $[0]_{n\times m}$ represents a zero-matrix of the indicated dimensions, I_n is the identity matrix of order n, and $[1]_{n\times 1}$ denotes a vector of dimension n with all its entries equal to 1. Next, we consider the vector of interstory drifts

$$x_r(t) = [q_1, q_2 - q_1, q_3 - q_2, q_4 - q_3, q_5 - q_4]^T, \quad (53)$$

and define the new state vector

$$x(t) = \begin{bmatrix} x_r(t) \\ \dot{x}_r(t) \end{bmatrix}, \quad (54)$$

which can be expressed as

$$x(t) = \mathcal{C} x_{_I}(t) \quad (55)$$

with

$$\mathcal{C} = \begin{bmatrix} 1 & 0 & 0 & 0 & 0 & 0 & 0 & 0 & 0 & 0 \\ -1 & 1 & 0 & 0 & 0 & 0 & 0 & 0 & 0 & 0 \\ 0 & -1 & 1 & 0 & 0 & 0 & 0 & 0 & 0 & 0 \\ 0 & 0 & -1 & 1 & 0 & 0 & 0 & 0 & 0 & 0 \\ 0 & 0 & 0 & -1 & 1 & 0 & 0 & 0 & 0 & 0 \\ 0 & 0 & 0 & 0 & 0 & 1 & 0 & 0 & 0 & 0 \\ 0 & 0 & 0 & 0 & 0 & -1 & 1 & 0 & 0 & 0 \\ 0 & 0 & 0 & 0 & 0 & 0 & -1 & 1 & 0 & 0 \\ 0 & 0 & 0 & 0 & 0 & 0 & 0 & -1 & 1 & 0 \\ 0 & 0 & 0 & 0 & 0 & 0 & 0 & 0 & -1 & 1 \end{bmatrix}. \quad (56)$$

The new state-space model is

$$S : \dot{x}(t) = Ax(t) + Bu(t) + Ew(t), \quad (57)$$

with

$$A = \mathcal{C} A_{_I} \mathcal{C}^{-1}, \quad B = \mathcal{C} B_{_I}, \quad E = \mathcal{C} E_{_I}. \quad (58)$$

The particular values of the matrices A, B and E are presented in Figure 5.

4.2 State-feedback H_∞ controller design

In this subsection, we assume that the actuation devices a_i displayed in Figure 4(b) are ideal force actuators and we design a state-feedback H_∞ controller

$$u(t) = G_s\, x(t) \quad (59)$$

to drive the actuation system. By setting the output matrix $C_y = I_{10}$ in eq. (21), the control design methodology discussed in Section 3 can be applied to compute the control gain matrix G_s. Note that the difficulties discussed in Remark 2 do not apply to this particular case, and solving the convex optimization problem

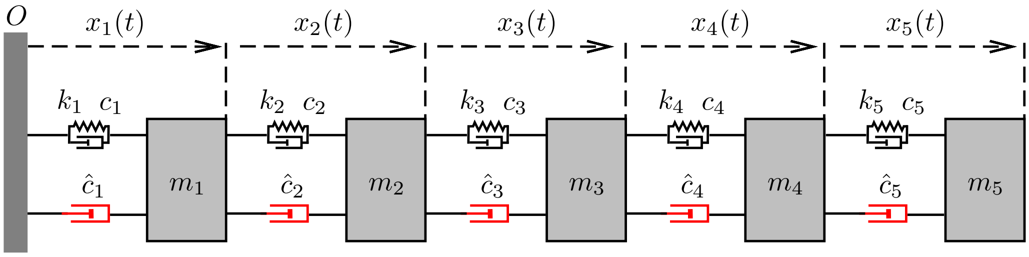

Figure 7: Five-degree-of-freedom mass-spring-damper representation of the five-story building with passive-damping actuation system

given in eq. (32) leads to the equation

$$\tilde{Y} = G_s \tilde{X}, \tag{60}$$

which can be easily solved for G_s, resulting

$$G_s = \tilde{Y} \left(\tilde{X}\right)^{-1}. \tag{61}$$

For the controlled-output matrices

$$C_z = \begin{bmatrix} I_{10} \\ [0]_{5\times 10} \end{bmatrix}, \quad D_z = 10^{-6.25} \times \begin{bmatrix} 0_{10\times 5} \\ I_5 \end{bmatrix}, \tag{62}$$

the optimization problem in eq. (32) produces the control gain matrix G_s displayed in Figure 6 with H_∞-norm

$$\gamma_{G_s} = 0.8266. \tag{63}$$

Remark 7 As indicated in Section 2, note that a practical implementation of the state-feedback controller $u(t) = G_s x(t)$ would require sensors of interstory drifts and interstory velocities, and also a full communication system.

4.3 Design of the passive damping system

Now, let us assume that the actuation devices a_i in Figure 4(b) are passive dampers with adjustable damping constants $\hat{c}_i$. Looking at the representation of the five-story building model as a five-degree-of-freedom mass-spring-damper system displayed in Figure 7, and considering the discussion in Section 2, it follows that the passive damping system can be suitably tuned by designing a decentralized velocity-feedback controller

$$u(t) = G_d\, y(t) \tag{64}$$

with

$$y(t) = \dot{x}_r(t), \tag{65}$$

and taking the damping constants

$$\hat{c}_i = -[g_d]_{ii}, \quad 1 \le i \le 5, \tag{66}$$

where $[g_d]_{ii}$ are the elements of the diagonal matrix G_d. To this end, we consider the model in eq. (21) with the output matrix

$$C_y = \left[[0]_{5\times 5}\ I_5\right], \tag{67}$$

together with the matrices C_z and D_z given in eq. (62). Next, we solve the optimization problem given in eq. (38) constraining the LMI matrices X_R and Y_R to diagonal form in order to compute a diagonal gain matrix G_d.

A first attempt at solving the LMI optimization problem with the *Matlab Robust Control Toolbox* [Balas et al. (2011)] fails, and the problem is reported to be infeasible. However, as pointed out in Rubió-Massegú et al. (2012a), this difficulty can be conveniently circumvented by adding a small perturbation to the system matrix. Using the perturbed state matrix

$$\hat{A} = A + \Delta A, \tag{68}$$

with

$$\Delta A = -0.01 \times I_{10}, \tag{69}$$

the following decentralized velocity-feedback control matrix results:

$$G_d = 10^6 \times \begin{bmatrix} -6.506 & 0 & 0 & 0 & 0 \\ 0 & -4.343 & 0 & 0 & 0 \\ 0 & 0 & -3.455 & 0 & 0 \\ 0 & 0 & 0 & -2.914 & 0 \\ 0 & 0 & 0 & 0 & -2.648 \end{bmatrix}, \tag{70}$$

which, according to the discussion in Section 2, defines a passive damping system with damping constants

$$\hat{c}_1 = 6.506 \times 10^6,\ \hat{c}_2 = 4.343 \times 10^6,\ \hat{c}_3 = 3.455 \times 10^6$$
$$\hat{c}_4 = 2.914 \times 10^6,\ \hat{c}_5 = 2.648 \times 10^6. \tag{71}$$

The optimal γ-value obtained in the solution of the LMI optimization problem is

$$\gamma_d = (\tilde{\eta}_{\mathrm{opt}})^{-1/2} = 0.8642. \tag{72}$$

This means that the H_∞-norm of the passive damping system is only about a 5% greater than the value

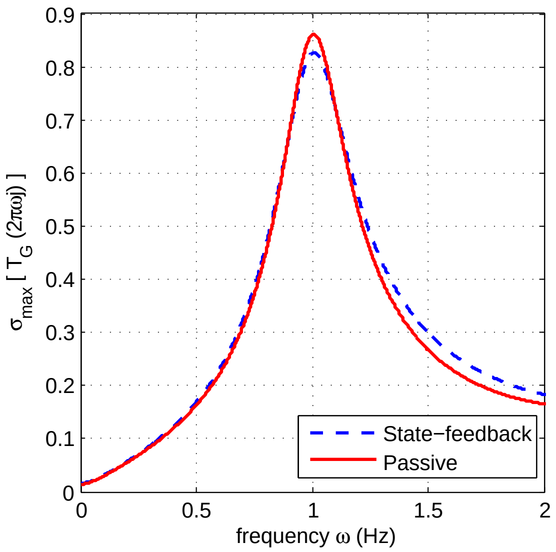

Figure 8: Maximum singular values for $T_G(j\omega)$

corresponding to the state-feedback controller. The excellent behavior of the passive damping system can be clearly appreciated in the graphics of maximum singular values of the pulse transfer functions $T_{G_s}(j\omega)$ (blue dashed line) and $T_{G_d}(j\omega)$ (red solid line) displayed in Figure 8.

Remark 8 The initial infeasibility of the LMI optimization problems associated to the design of static output-feedback controllers for structural vibration control is a strange and poorly understood phenomenon. From a practical perspective, extensive numerical simulations show that using a perturbed state matrix in the form given in eqs. (68) and (69) is a very effective strategy to overcome the problem. A more general formulation of the transformations given in eq. (37) has been recently presented in Rubió-Masseguú et al. (2012b), which can help to provide a more satisfactory solution to this feasibility problem.

Remark 9 As indicated in Remark 6, the value γ_d in eq. (72) is an upper bound of the H_∞-norm γ_{G_d}. The actual value of γ_{G_d}, computed from eq. (28), is $\gamma_{G_d} = 0.8609$. This value corresponds to the peak of the red solid line in Figure 8.

4.4 Numerical simulations

In this subsection, the full-scale North-South 1968 Hachinohe seismic record (see Figure 9) is used as ground acceleration input to carry out numerical simulations of the free and controlled responses of the five-story building. In Figure 10, the upper graphic shows the maximum absolute interstory drifts obtained for three different configurations: (i) uncontrolled building (black squares), (ii) controlled building with ideal

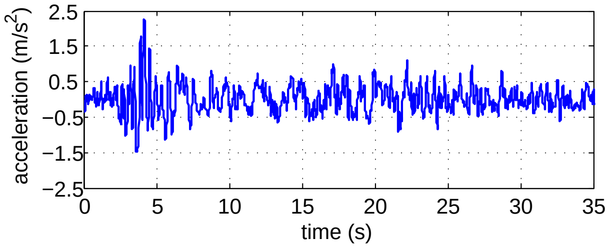

Figure 9: Full-scale North–South 1968 Hachinohe seismic record

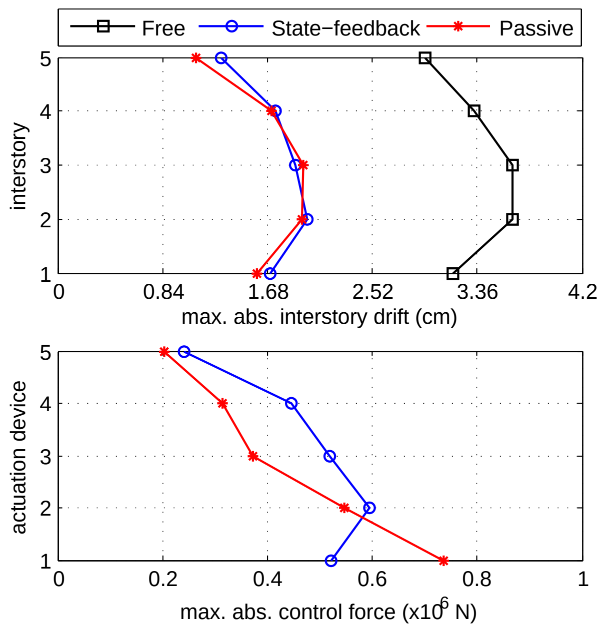

Figure 10: Maximum absolute interstory drifts and control efforts

force actuation devices driven by the centralized state-feedback controller defined by the gain matrix G_s (blue circles), and (iii) controlled building with the passive damping system defined by the damping constants given in eq. (71) (red asterisks). These configurations are denoted in the legend as *Free*, *State-feedback* and *Passive*, respectively. The corresponding maximum absolute actuation forces are displayed in the lower graphic using the same symbols and colors.

Together with the typical good behavior of the state-feedback H_∞ controllers, the graphics show that the passive damping system achieves practically the same maximum absolute interstory drifts as the state-feedback controller, requiring also similar levels of control effort. The behavior exhibited by the passive damping system is certainly remarkable, especially if we take into account that it can operate without sensors, with null power requirements, and no communication system.

5 Conclusions and future directions

In this work, a new strategy to design passive energy dissipation systems for vibration control of large structures has been presented. The method is based on the equivalence between passive damping systems and fully decentralized static velocity-feedback controllers. Using recent developments in static output-feedback control design, the constants of the passive dampers can be computed by solving a single optimization problem with Linear Matrix Inequality constraints. The application of the proposed methodology has been illustrated by designing a passive energy dissipation system for seismic protection of a five-story building. Numerical simulations of the building vibrational response confirm the excellent behavior of the proposed passive damping system.

It should be highlighted that the new approach can be of interest in a wide variety of research fields where the mitigation of undesirable vibrational responses is a major concern. Examples of practical interest can be found, for instance, in seismic protection of multi-building systems [Yang et al. (2003), Matsagar and Jangid (2005), Bhaskararao and Jangid (2006), Kim et al. (2006), Bharti et al. (2010), Zhu et al. (2011), Palacios-Quiñonero et al. (2012c)], automotive industry [Zhang et al. (2011a), Li et al. (2012a), Zapateiro et al. (2012)], or offshore wind power generation [Colwell and Basu (2009), Li et al. (2012b)]. Consequently, further research effort needs to be aimed at exploring additional applications of the proposed methodology.

Acknowledgments

This work has been partially supported by the Spanish Ministry of Economy and Competitiveness through the grant DPI2011-27567-C02, and by the Norwegian Center of Offshore Wind Energy (NORCOWE) under grant 193821/S60 from the Research Council of Norway (RCN). NORCOWE is a consortium with partners from industry and science, hosted by Christian Michelsen Research.

References

Agrawal, A. and Yang, J. Design of passive energy dissipation systems based on LQR control methods. *Journal of Intelligent Material Systems and Structures*, 1999. 10(12):933–944. doi:10.1106/FB58-N1DG-ECJT-B8H4.

Balas, G., Chiang, R., Packard, A., and Safonov, M. *MATLAB^{TM} Robust Control Toolbox^{TM} 3. User's Guide*. The MathsWorks, Inc., 3 Apple Hill Drive. Natick, MA 01760–20, USA, 2011.

Bharti, S., Dumne, S., and Shrimali, M. Seismic response analysis of adjacent buildings connected with MR dampers. *Engineering Structures*, 2010. 32(8):2122–2133. doi:10.1016/j.engstruct.2010.03.015.

Bhaskararao, A. and Jangid, R. Seismic response of adjacent buildings connected with friction dampers. *Bulletin of Earthquake Engineering*, 2006. 4(1):43–64. doi:10.1007/s10518-005-5410-1.

Boyd, S., Ghaoui, L. E., Feron, E., and Balakrishnan, V. *Linear Matrix Inequalities in System and Control Theory*. SIAM Studies in Applied Mathematics, Philadelphia, USA, 1994.

Chen, Y., Zhang, W., and Gao, H. Finite frequency H_∞ control for building under earthquake excitation. *Mechatronics*, 2010. 20(1):128–142. doi:10.1016/j.mechatronics.2009.11.001.

Chopra, A. *Dynamics of Structures. Theory and Applications to Earthquake Engineering*. Prentice Hall, Upper Saddle River, New Jersey, USA, 3rd edition, 2007.

Colwell, S. and Basu, B. Tuned liquid column dampers in offshore wind turbines for structural control. *Engineering Structures*, 2009. 31(2):358–368. doi:10.1016/j.engstruct.2008.09.001.

Du, H. and Lam, J. Energy-to-peak performance controller design for building via static output feedback under consideration of actuator saturation. *Computers & Structures*, 2006. 84(31–32):2277–2290. doi:10.1016/j.compstruc.2006.08.032.

Gluck, N., Reinhorn, A., Gluck, J., and Levy, R. Design of supplemental dampers for control of structures. *Journal of Structural Engineering*, 1996. 122(12):1394–1399. doi:10.1061/(ASCE)0733-9445(1996)122:12(1394).

Ikeda, Y. Active and semi-active vibration control of buildings in Japan – Practical applications and verification. *Structural Control and Health Monotoring*, 2009. 16(8):703–723. doi:10.1002/stc.315.

Kim, J., Ryu, J., and Chung, L. Seismic performance of structures connected by viscoelastic dampers. *Engineering Structures*, 2006. 28(2):183–195. doi:10.1016/j.engstruct.2005.05.014.

Kurata, N., Kobori, T., Takahashi, M., Niwa, N., and Midorikawa, H. Actual seismic response controlled building with semi-active damper system. *Earthquake Engineering and Structural Dynamics*, 1999. 28(11):1427–1447.

Li, H. and Huo, L. Advances in structural control in civil engineering in China. *Mathematical Problems in Engineering*, 2010. 2010:1–23. doi:10.1155/2010/936081.

Li, H., Liu, H., Gao, H., and Shi, P. Reliable fuzzy control for active suspension systems with actuator delay and fault. *IEEE Transactions on Fuzzy Systems*, 2012a. 20(2):342–357. doi:10.1109/TFUZZ.2011.2174244.

Li, J., Zhang, Z., and Chen, J. Experimental study on vibration control of offshore wind turbines usign a ball vibration absorber. *Energy and Power Engineering*, 2012b. 4:153–157. doi:10.4236/epe.2012.43021.

Matsagar, V. and Jangid, R. Viscoelastic damper connected to adjacent structures involving seismic isolation. *Journal of Civil Engineering and Management*, 2005. 11(4):309–322. doi:10.1080/13923730.2005.9636362.

Palacios-Quiñonero, F., Rossell, J., and Karimi, H. Semi-decentralized strategies in structural vibration control. *Modeling, Identification and Control*, 2011. 32(2):57–77. doi:10.4173/mic.2011.2.2.

Palacios-Quiñonero, F., Rossell, J., Rubió-Massegú, J., and Karimi, H. Structural vibration control for a class of connected multistructure mechanical systems. *Mathematical Problems in Engineering*, 2012a. 2012:1–23. doi:10.1155/2012/942910.

Palacios-Quiñonero, F., Rubió-Masseguú, J., Rossell, J., and Karimi, H. Discrete-time multioverlapping controller design for structural vibration control of tall buildings under seismic excitation. *Mathematical Problems in Engineering*, 2012b. 2012:1–20. doi:10.1155/2012/636878.

Palacios-Quiñonero, F., Rubió-Massegú, J., Rossell, J., and Karimi, H. Semiactive-passive structural vibration control strategy for adjacent structures under seismic excitation. *Journal of the Franklin Institute*, 2012c. 349:3003–3026. doi:10.1016/j.jfranklin.2012.09.005.

Rubió-Massegú, J., Palacios-Quiñonero, F., and Rossell, J. Decentralized static output-feedback H_∞ controller design for buildings under seismic excitation. *Earthquake Engineering and Structural Dynamics*, 2012a. 41:1199–1205. doi:10.1002/eqe.1167.

Rubió-Massegú, J., Rossell, J., Karimi, H., and Palacios-Quiñonero, F. Static output-feedback control under information structure constraints. *Automatica*, 2012b. In press:1–4 doi:10.1016/j.automatica.2012.10.012.

Spencer, B. and Nagarajaiah, S. State of the art of structural control. *Journal of Structural Engineering*, 2003. 129(7):845–856. doi:10.1061/(ASCE)0733-9445(2003)129:7(845).

Swartz, R. and Lynch, J. Strategic network utilization in a wireless structural control system for seismically excited structures. *Journal of Structural Engineering*, 2009. 135(5):597–608. doi:10.1061/(ASCE)ST.1943-541X.0000002.

Yang, J., Lin, S., Kim, J.-H., and Agrawal, A. Optimal design of passive energy dissipation systems based on H_∞ and H_2 performances. *Earthquake Engineering and Structural Dynamics*, 2002. 31(4):921–936. doi:10.1002/eqe.130.

Yang, Z., Xu, Y., and Lu, X. Experimental seismic study of adjacent buildings with fluid dampers. *Journal of Structural Engineering*, 2003. 129(2):197–205. doi:10.1061/(ASCE)0733-9445(2003)129:2(197).

Zapateiro, M., Pozo, F., Karimi, H., and Luo, N. Semiactive control methodologies for suspension control with magnetorheological dampers. *IEEE/ASME Transactions on Mechatronics*, 2012. 17(2):370–380. doi:10.1109/TMECH.2011.2107331.

Zhang, H., Shi, Y., and Mehr, A. Robust non-fragile dynamic vibration absorbers with uncertain factors. *Journal of Sound and Vibration*, 2011a. 330(4):559–566. doi:10.1016/j.jsv.2010.10.012.

Zhang, W., Chen, Y., and Gao, H. Energy-to-peak control for seismic-excited buildings with actuator faults and parameter uncertainties. *Journal of Sound and Vibration*, 2011b. 330(4):581–602. doi:10.1016/j.jsv.2010.09.001.

Zhu, H., Ge, D., and Huang, X. Optimum connecting dampers to reduce the seismic responses of parallel structures. *Journal of Sound and Vibration*, 2011. 330(9):1931–1949. doi:10.1016/j.jsv.2010.11.016.